

volume 104  
number D16

AUGUST 27, 1999

Journal of  
Geophysical  
Research



PUBLISHED BY AMERICAN GEOPHYSICAL UNION

Including Special Section:

GEWEX Continental-Scale  
International Project (GCIP), Part 2

## A parameterization of snowpack and frozen ground intended for NCEP weather and climate models

V. Koren,<sup>1</sup> J. Schaake,<sup>1</sup> K. Mitchell,<sup>2</sup> Q.-Y. Duan,<sup>1</sup> F. Chen,<sup>3</sup> J. M. Baker<sup>4</sup>

**Abstract.** Extensions to the land surface scheme (LSS) in the National Centers for Environmental Prediction, regional, coupled, land-atmosphere weather prediction model, known as the mesoscale Eta model, are proposed and tested off-line in uncoupled mode to account for seasonal freezing and thawing of soils and snow-accumulation–ablation processes. An original model assumption that there is no significant heat transfer during redistribution of liquid water was relaxed by including a source/sink term in the heat transfer equation to account for latent heat during phase transitions of soil moisture. The parameterization uses the layer-integrated form of heat and water diffusion equations adopted by the original Eta-LSS. Therefore it simulates the total ice content of each selected soil layer. Infiltration reduction under frozen ground conditions was estimated by probabilistic averaging of spatially variable ice content of the soil profile. Off-line uncoupled tests of the new and original Eta-LSS were performed using experimental data from Rosemount, Minnesota. Simulated soil temperature and unfrozen water content matched observed data reasonably well. Neglecting frozen ground processes leads to significant underestimation/overestimation of soil temperature during soil freezing/thawing periods and underestimates total soil moisture content after extensive periods of soil freezing.

### 1. Introduction

Winter season processes significantly influence water and heat fluxes between the atmospheric boundary layer and the land surface in both the real world and in the coupled land-atmosphere models. There is empirical evidence that thermodynamic effects of variable snow cover over North America alter temperature anomalies and precipitation patterns over the contiguous United States [Namias, 1985] and that changes in snow cover over Eurasia affect the monsoon strength [Barnett *et al.*, 1989]. From a climate model study, Yeh *et al.* [1983] found that fast removal of snow cover can produce a hydrological climatic effect that can last as long as 4–5 months. Frozen ground and snow cover also influence rainfall-runoff partitioning, the timing of spring runoff, and the amount of soil moisture that subsequently is available for evapotranspiration in spring and summer. Nearly impermeable soil layers can develop because soil may freeze during winter and spring seasons. Finally, on shorter timescales, frozen ground and snow cover can strongly influence the diurnal surface heat fluxes on daily timescales, thereby affecting the near-surface atmospheric temperature forecasts in numerical weather prediction (NWP) models. This present work was partly motivated by a systematic midday near-surface cold bias over a shallow melting snowpack in the coupled Eta NWP model: a bias arising from a lack of subgrid “patchiness” treatment for the shallow

snow which acts to suppress skin temperature and upward surface heat flux. Such a low-level temperature bias can, for example, adversely effect the outlook for precipitation type (rain, freezing rain, sleet, snow).

Some effects of winter season surface processes on runoff and land surface temperature can be seen from the following two examples: Figure 1 illustrates the effect of frozen soil on precipitation-runoff partitioning during flood events on the Root River basin, Minnesota, where frozen soil depth can be as much as 2 m. The same precipitation amount when the soil is frozen in winter and spring produces much more runoff than when the soil is not frozen. As shown in the figure, antecedent soil moisture conditions alone cannot explain these differences. Observations from the Rosemount site of the Minnesota Agricultural Experimental Station [Spaans and Baker, 1996] in Figure 2 show that upper layer soil temperatures vary differently when air temperature is above freezing than when below freezing. There is a strong correlation when air temperatures are above freezing but little correlation when there is frozen soil or snow cover.

There has been much theoretical and field investigation of cold season processes at small plot scales [e.g., Anderson, 1976; Kane and Stein, 1983; Motovilov, 1986; Lunardini, 1988; Levine and Knoz, 1997]. Unfortunately, field experiments historically have been limited to the plot scale and have not produced information about spatial variability that is needed to apply basic physical models appropriate at the plot scale to large spatial scales where spatial heterogeneity of these processes must be considered. Much of the past large-scale research has not treated this heterogeneity explicitly and has produced very simple, conceptual parameterizations of the snow cover and frozen ground [e.g., Anderson, 1973; Bergstrom, 1975; DeGaetano *et al.*, 1996].

The high sensitivity of weather and climate systems to winter and summer land surface forcing has created a recent interest in upgrading the cold and warm season land surface param-

<sup>1</sup>Office of Hydrology, National Weather Service/NOAA, Silver Spring, Maryland.

<sup>2</sup>National Centers for Environmental Prediction/NOAA, Camp Springs, Maryland.

<sup>3</sup>National Center for Atmospheric Research, Boulder, Colorado.

<sup>4</sup>Department of Soil, Water, and Climate, University of Minnesota, St. Paul.

Copyright 1999 by the American Geophysical Union.

Paper number 1999JD900232.

0148-0227/99/1999JD900232\$09.00

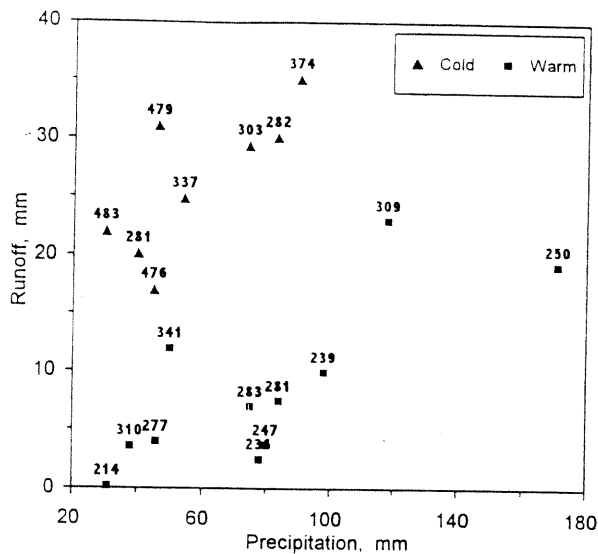


Figure 1. Precipitation-runoff relationship during periods when soil is estimated to be frozen or unfrozen. Points are labeled with soil moisture depth in millimeters.

eterizations of atmospheric models [Verseghy, 1991; Dickinson *et al.*, 1993; Marshall *et al.*, 1994; Lynch-Stieglitz, 1995; Foster *et al.*, 1996]. A high priority objective of the Global Water and Energy Experiment (GEWEX) Continental-Scale International Project (GCIP) is to improve the representation of cold season processes in climate and weather models [Leese, 1997]. Achieving this objective is difficult because it is not possible to make all of the detailed measurements that ideally would be needed to explicitly validate all of the assumptions required to account for the large-scale effects of heterogeneity in the basic physical processes. The National Centers for Environmental Prediction (NCEP) (formerly the National Meteorological Center) develops and executes a suite of regional and global weather prediction models (1–14 days) and climate prediction models (1–12 months), as summarized by McPherson [1994]. The weather prediction models, such as the regional Eta model [Black, 1994], represent coupled land-atmosphere physical systems that include soil moisture/temperature and snowpack as predicted state variables. The climate prediction models [Ming *et al.*, 1994] additionally include a coupled ocean component that predicts sea surface temperature. In collaboration with the GCIP community, the Office of Hydrology and NCEP are jointly pursuing improvements to the NCEP LSS. Such improvements are first tested off-line in an uncoupled mode, such as in the present study, then implemented in the regional coupled Eta model, followed by implementation in the global models.

The objectives of the present off-line uncoupled study are (1) to improve the Eta-LSS by considering snow and frozen ground processes not included in the existing LSS as well as the spatial variability of these processes and (2) to begin to close the gap between model development and validation by testing the new parameterization using data from a plot scale field experiment at Rosemount, Minnesota. Additional tests at larger spatial scales are planned for the future using PILPS phase 2d forcing data from Valday Russia [Schlosser *et al.*, 1997] and for a number of natural river basins in the Upper Mississippi basin.

## 2. Snow-Frozen Ground Parameterization Development

This study presents extensions of the Eta-LSS that include the effects of frozen ground, patchy snow cover, and temporal/spatial variability in snow properties. These extensions were developed so that the added physical complexity and soil profile treatment are compatible with general complexity and configuration of the present Eta model. Accordingly, a physically based parameterization of frozen ground and a more realistic snow accumulation-ablation scheme were introduced. An original model assumption that there is no significant heat transfer during redistribution of liquid water between soil layers was relaxed by including a source/sink term in the heat transfer equation to account for the latent heat during phase transitions of soil moisture.

### 2.1. Original Eta Model Land-Surface Parameterization

The Eta-LSS [Chen *et al.*, 1997, Appendix B] employs the National Weather Service (NWS) National Centers for Environmental Prediction (NCEP) and Office of Hydrology (OH) extensions to the multilayer OSU (Oregon State University) soil/vegetation scheme [Pan and Mahrt, 1987; Ek and Mahrt, 1991]. It couples the Penman potential evaporation approach of Mahrt and Ek [1984], the multilayer soil model of Mahrt and Pan [1984], the canopy resistance-based model of Ek and Mahrt [1991], and the surface runoff component from the SWB model [Schaake *et al.*, 1996].

The surface energy and water budgets are computed for a single unified ground-vegetation surface. Soil moisture and heat fluxes are simulated separately at each time step, assuming no significant heat transfer during redistribution of liquid water [Taylor and Luthin, 1976]. The existing parameterization does not account for the latent heat of soil moisture phase transitions, assuming instead that water is liquid at any temperature. Ground heat flux is controlled by the diffusion equation for soil temperature  $T$  [Chen *et al.*, 1996]

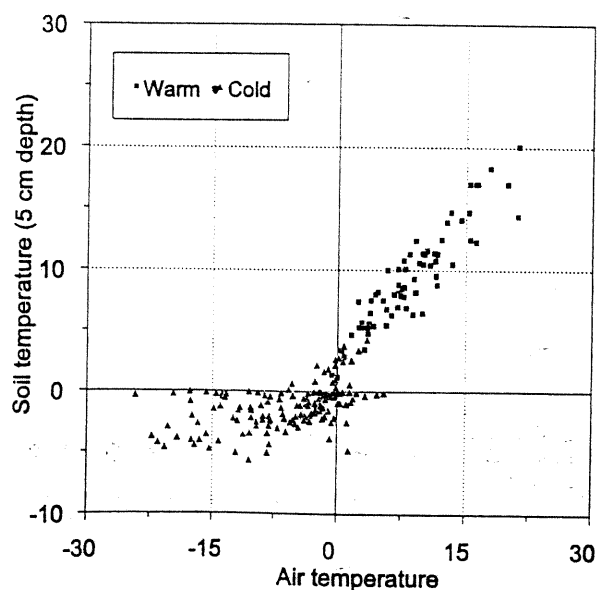


Figure 2. Soil-air temperature relationship at the Rosemount site.

$$C(\theta) \frac{\partial T}{\partial t} = \frac{\partial}{\partial z} \left[ K(\theta) \frac{\partial T}{\partial z} \right] \quad (1)$$

where the volumetric heat capacity  $C$  and the thermal conductivity  $K$  are formulated as functions of volumetric soil moisture content  $\theta$ . Equation (1) does not include latent heat flux of evaporation explicitly. Rather, it is accounted for by the upper boundary condition of ground-vegetation surface skin temperature, obtained via the surface energy balance equation that includes latent heat of evaporation. Soil temperature at the lower boundary (usually at 3 m depth) is assumed to be constant at the long-term mean annual air temperature.

The diffusive form of Richard's equation is used to predict volumetric soil moisture content:

$$\frac{\partial \theta}{\partial t} = \frac{\partial}{\partial z} \left[ D(\theta) \frac{\partial \theta}{\partial z} + K_w(\theta) \right] + F_w(\theta) \quad (2)$$

where the soil water diffusivity  $D$  and hydraulic conductivity  $K_w$  are functions of volumetric soil moisture content, and the source/sink of soil water  $F_w$  represents effects of infiltration and evaporation. Water diffusivity is given by  $D(\theta) = K_w(\theta) [\partial \Psi / \partial \theta]$ , wherein  $\Psi$  is the soil water potential. Campbell's [1974] approximations for  $K_w$  and  $\Psi$ , as given by  $K_w(\theta) = K_w(\theta_s) (\theta/\theta_s)^{2b+3}$  and  $\Psi = \Psi_s (\theta/\theta_s)^{-b}$ , were used in the parameterization. Saturated volumetric water content  $\theta_s$ , hydraulic conductivity  $K_w(\theta_s)$ , water potential  $\Psi_s$ , and parameter  $b$  are estimated on the basis of field measurements of soil properties if available, or on the basis of empirical values dependent on soil classification [Cosby et al., 1984].

Evaporation from the ground-vegetation surface is the sum of the direct evaporation  $E_1$  from the top soil layer, evaporation of precipitation intercepted by the canopy  $E_c$ , and transpiration  $E_t$ . Direct evaporation from the first soil layer is given by the so-called linear "Beta" method [Mahfouf and Noilhan, 1991], namely  $E_{dir} = \beta * E_p$ , where  $\beta$  is the fraction of soil moisture relative to an upper limit moist reference value such as field capacity. An application of this formulation to the NCEP Eta model is described by Betts et al. [1997]. A formulation similar to Jacquemin and Noilhan [1990] is used for the wet canopy evaporation  $E_c$ . Transpiration  $E_t$  is assumed to be proportional to the potential evaporation and inversely related to canopy resistance. Jarvis [1976] parameterization of the canopy resistance is used. The green vegetation fraction [Gutman and Ignatov, 1998] acts as a weighting factor among the three components. Total evaporation and its components are bounded by the potential evaporation from a Penman-based energy balance approach [Mahrt and Ek, 1984].

The layer-integrated forms of (1) and (2) are solved using the implicit Crank-Nicholson scheme [Pan and Mahrt, 1987]. Solutions to (1) and (2) are assumed to represent soil temperature and soil moisture values located at the middle point of each soil layer. Although two-four layers that extend at least over the root zone have been used in different applications, more layers could be easily accommodated.

The boundary condition of water input at the top layer is the excess precipitation after canopy abstraction plus snowmelt  $P_x$ , less surface runoff  $R_s$ , and direct evaporation  $E_1$  and transpiration from the top soil layer  $E_{t,1}$ . The SWB formulation [Schaake et al., 1996] is used to specify surface runoff. Losses due to transpiration are the only source/sink term of other root zone layers. It is assumed that the total transpiration  $E_t$  is partitioned between root zone layers according to the layer

weights  $\chi_i = \Delta z_i / z_r$ , where  $\Delta z_i$  is the depth of  $i$ th layer and  $z_r$  is the total rooting depth. "Gravitational" percolation  $K_w(\theta_b)$  is the lower boundary condition. There is no water diffusion at the lower boundary. A more detailed description of the Eta-LSS is given by Chen et al. [1996].

Snow accumulation/ablation parameterization of the original Eta model [Chen et al., 1996] is based on the energy and mass balance of the snowpack:

$$\frac{dW_s}{dt} = P_s - M_s - E \quad (3)$$

$$M_s = \frac{1}{L} (Q_{sw} + Q_{lw} - Q_{lt} - Q_{sn} - Q_g) \quad (4)$$

where  $W_s$  is the snow water equivalent,  $P_s$  is precipitation in the form of snow,  $M_s$  is the snowmelt rate,  $E$  is the snow evaporation,  $Q_{sw}$  is net solar radiation,  $Q_{lw}$  is net longwave radiation,  $Q_{lt}$  is the latent heat flux,  $Q_{sn}$  is the sensible heat flux,  $Q_g$  is ground head flux, and  $L$  is the latent heat of fusion. The parameterization neglects heat transferred by movement of meltwater in the snowpack and assumes that all liquid water immediately reaches the soil. It also neglects fractional snow-covered area (except for the snow albedo). Snowpack physical characteristics, thermal conductivity  $K_s$ , and density  $\rho_s$  are assumed constant at  $0.35 \text{ W m}^{-1} \text{ K}^{-1}$  and  $0.1 \text{ g cm}^{-3}$ , respectively. Below, it will be shown that this assumption can lead to significant overestimation of snow depth.

## 2.2. Improvements to Snowpack Parameterization

Although the original Eta-LSS accounts reasonably well for heat fluxes at the snow surface and for the accumulated amount of snow water, overestimation of snow depth, and snow area can cause biases in snow-soil surface heat exchange. A snow compaction parameterization was introduced to overcome this problem. On the basis of the Kojima [1967] model of snow compaction, Anderson [1976] proposed an expression for snow density change due to compaction

$$\frac{1}{\rho_s(z)} \frac{d\rho_s(z)}{dt} = C_1 W_s(z) e^{0.087(T_s(z) - C_2 \rho_s(z))} \quad (5)$$

where snow density  $\rho_s(z)$  increases depending on snow water amount above level  $z$  and snow temperature  $T_s(z)$  at that level.  $C_1$  is the fractional increase in density per unit water equivalent of load per unit time at zero temperature and density.  $C_2$  is a constant determined from observed data.

To apply (5) directly, the snowpack must be divided into many layers, which would be computationally too expensive to be used in the present Eta model. Because the right-hand term of (5) is nearly constant within each time step (usually 5–15 min), an approximate solution of (5) can be derived:

$$\rho_{s,t+\Delta t}(z) = \rho_{s,t}(z) \exp [C_1 \Delta t W_s(z) e^{0.087(T_s(z) - C_2 \rho_{s,t}(z))}] \quad (6)$$

Average snow density of the snowpack may be expressed as an integral of (6) over the snow depth  $H$ :

$$\rho_{s,t+\Delta t} = \rho_{s,t} \frac{e^{B W_{s,t}} - 1}{B W_{s,t}} \quad (7)$$

where

$$B = \Delta t C_1 e^{0.087(T_s - C_2 \rho_{s,t})} \quad (8)$$

Kojima [1967] reported a value of  $0.026 \text{ cm}^{-1} \text{ h}^{-1}$  for  $C_1$ , and a value of  $21 \text{ cm}^{-3} \text{ g}^{-1}$  for  $C_2$ ; snow density is expressed in  $\text{g cm}^{-3}$  and snow water equivalent in centimeters. However, Anderson's [1976] analysis of extensive experimental data in Vermont indicated that the  $C_1$  value reported by Kojima was too high. He suggested a value of  $0.01 \text{ cm}^{-1} \text{ h}^{-1}$ .

Since snowmelt and new snowfall also affect snow density and depth, snow density during snowfall/snowmelt is adjusted according to the following expression:

$$\rho_{s,t+dt} = \min \left[ \frac{\rho_{s,t}(W_{s,t} - 0.87 M_t) + 0.13 \rho_w M_s + \rho_{\text{new}} W_{\text{new}}}{W_{s,t} + 0.13 M_s + W_{\text{new}}}, 0.40 \right] \quad (9)$$

where  $W_{\text{new}}$  is the water equivalent of new snowfall,  $\rho_w$  is the water density, and  $\rho_{\text{new}}$  is the density of new snowfall, which can be estimated on the basis of air temperature  $T_{\text{air}}$  [Gottlieb, 1980]

$$\rho_{\text{new}} = \max [0.05 + 0.0017(T_{\text{air}} + 15)^{1.5}, 0.05], \text{ g cm}^{-3} \quad (10)$$

Equation (9) assumes that 13% of snowmelt water can be stored in snowpack [Koren, 1991]. Snow density is bounded by a  $0.4 \text{ g cm}^{-3}$  upper limit. An exponential function with an upper bound limit  $W_{\text{max}}$  was used to account for the fractional snow coverage  $f$ :

$$f \left( \frac{W_s}{W_{\text{max}}} \right) = \alpha_s \frac{W_s}{W_{\text{max}}} e^{-\alpha_s(W_s/W_{\text{max}})} + \frac{1}{W_{\text{max}}} e^{-\alpha_s} \quad (11)$$

where  $\alpha_s$  is a distribution shape parameter. Equation (11) fits Anderson's [1973] empirical areal snow depletion curves well for  $\alpha_s$  varying from 2 to 4.

Because the current Eta-LSS uses a single snow-soil interface temperature and assumes a constant 100% snow cover area, it cannot account for the influence of subgrid bare patches of soil on the skin temperature of the unified surface. Hence the skin temperature during snowmelt never exceeds the melting point. In the new scheme, the skin temperature during snowmelt is weighted, according to the fractional snow coverage of (11), between the melting point and the skin temperature estimated for non-snow-covered surface.

### 2.3. New Frozen Ground Parameterization

A distinguishing feature of frozen ground processes is the formation of practically impermeable soil layers, or in extreme circumstances frost heave, which cause a significant reduction of water infiltration during snowmelt periods [Komarov, 1957; O'Neill, 1983; Fukuda and Ishizaki, 1992; Sheng et al., 1995]. A number of frost heave models have been proposed (review of the existing models is given by O'Neill [1983] and Fukuda and Ishizaki [1992]) which are based on the thermodynamic equations of a soil column and do not account for the spatial heterogeneity of frozen ground conditions. Some parameters of these models are not readily available and are difficult to determine [Sheng et al., 1995] over the entire North American continental domain of the Eta model. In this study we combined a simplified thermodynamical approach to represent local (soil column) physical processes with a probabilistic representation of the spatial variability of the frozen ground conditions (the latter is defined in section 2.4).

The parameterization of local processes is based on the heat and moisture transfer equations. The following assumptions were made: (1) all water phases are in thermal equilibrium, (2) heat associated with convective water flow can be neglected [Taylor and Luthin, 1976], (3) liquid water flow in the frozen soil is analogous to that in unfrozen soil [Harlan, 1973], and (4) the same relations for matric potential and hydraulic conductivity can be used under both frozen and unfrozen conditions. Under these assumptions, Richard's equation (2) can be used to estimate unfrozen soil water movement in a soil column. The only difference is that the total soil moisture content should be replaced by unfrozen water content, and the surface runoff formulation should consider frozen soil.

To account for soil moisture phase transitions (latent heat of fusion), the heat flux equation (1) was replaced by a diffusion equation with a source/sink term [Engelmark and Svensson, 1993]:

$$C(\theta, \theta_{\text{ice}}) \frac{\partial T}{\partial t} = \frac{\partial}{\partial z} \left[ K(\theta, \theta_{\text{ice}}) \frac{\partial T}{\partial z} \right] + \rho L \frac{\partial \theta_{\text{ice}}}{\partial t} \quad (12)$$

where  $L$  is the latent heat of fusion, the volumetric heat capacity  $C$  and the thermal conductivity  $K$  are now functions of total volumetric soil moisture content  $\theta$  and volumetric ice content  $\theta_{\text{ice}}$  (note that unfrozen volumetric soil water is  $\theta - \theta_{\text{ice}}$ ). Volumetric heat capacity of soil is the sum of the volumetric heat capacities of the soil constituents

$$C(\theta, \theta_{\text{ice}}) = (\theta - \theta_{\text{ice}})C_w + \theta_{\text{ice}}C_{\text{ice}} + (\theta_s - \theta)C_{\text{air}} + (1 - \theta_s)C_{\text{soil}} \quad (13)$$

where  $C_w$ ,  $C_{\text{ice}}$ ,  $C_{\text{air}}$ , and  $C_{\text{soil}}$  are the volumetric heat capacities of water, ice, air, and soil minerals,  $\theta_s$  is the saturated volumetric total water content (unfrozen and frozen). Various methods have been developed to estimate thermal conductivity of frozen soils (see a comprehensive review by Farouki [1986]). The methods are purely empirical or semiempirical and include a number of widely variable parameters. None of these methods provide highly accurate estimates of thermal conductivity for various soil types [Farouki, 1986]. Furthermore, spatial variability of soil properties as well as that of thermal and saturation conditions can significantly increase the uncertainty of these estimates. To reduce the uncertainties, a simple linear equation suggested by Kutchment et al. [1983] is used to adjust thermal conductivity of unfrozen soil under frozen conditions:

$$K(\theta, \theta_{\text{ice}}) = K(\theta)(1 + \theta_{\text{ice}}) \quad (14)$$

where thermal conductivity  $K(\theta)$  for unfrozen soil is estimated from McCumber and Pielke [1981] relationship used in the original Eta-LSS, although the upper bound of thermal conductivity was restricted significantly to a value of  $1.9 \text{ W m}^{-1} \text{ K}^{-1}$ .

The implicit Crank-Nicholson scheme is also used to solve the layer-integrated form of (12). An explicit approximation is applied to the source/sink term. To reduce numerical error during fast freezing/thawing of soil, two iterations of (12) are used. This is similar to how water fluxes are simulated from (2) during rainfall events. The ice content at each soil layer is estimated as a function of soil temperature and total soil moisture content [Flerchinger and Saxton, 1989; Kulik, 1978]. It is assumed that when ice is present, soil water potential remains in equilibrium with the vapor pressure over pure ice. A simple relationship, based on the Clausius-Clapeyron equation for

phase equilibrium, can be drawn between the freezing point of soil water and the soil water potential  $\Psi$ , after neglecting soil water osmotic potential [Fuchs *et al.*, 1978]:

$$\Psi = \frac{LT}{g(T + 273.16)} \quad (15)$$

where soil temperature  $T$  is in Celsius degrees, and  $g$  is the acceleration of gravity. Campbell's relationship between water potential and water content was modified to account for the effects of frozen soils [Kulik, 1978]

$$\Psi(\theta, \theta_{ice}) = \Psi_s \left( \frac{\theta - \theta_{ice}}{\theta_s} \right)^{-b} (1 + c_k \theta_{ice})^2 \quad (16)$$

where parameter  $c_k$  accounts for the effect of increase in specific surface of soil minerals and ice-liquid water; Kulik [1978] reported an average value of 8 for this parameter.

Combining (15) and (16) leads to

$$\frac{g\Psi_s}{L} (1 + c_k \theta_{ice})^2 \left( \frac{\theta - \theta_{ice}}{\theta_s} \right)^{-b} - \frac{T}{T + 273.16} = 0 \quad (17)$$

Equation (17) indicates that the ice content is a function of both soil temperature and soil moisture content. This agrees with laboratory/field experiments [Faruqi, 1986].

Because the actual amount of water converted into ice or vice versa depends on available incoming heat flux, the actual amount of ice/water generated per each time interval may be less than the potential ice content estimated from (17). The actual increase/decrease of the volumetric ice content,  $\Delta\theta_{ice,j}^*$ , at  $j$ th soil layer for time interval  $\Delta t$  is equal to

$$\Delta\theta_{ice,j}^* = \min \left( \frac{q_{T,j}\Delta t}{\rho L \Delta z_j}, \Delta\theta_{ice,j} \right) \quad (18)$$

where  $q_{T,j}$  is the heat flux into the layer assuming that water phase transitions occur in the middle of each layer, and  $\Delta\theta_{ice,j}$  is the potential increase/decrease of ice content estimated from (17). This approach does not account explicitly for the freezing front propagation because the integrated form of the diffusion equation is used. Phase transitions can occur at each layer at the same time depending on the distribution of soil temperature and heat fluxes.

#### 2.4. Infiltration Reduction Under Frozen Ground Conditions

The original Eta-LSS simulates infiltration as a residual of the excess precipitation after canopy abstraction  $P_x$  and sur-

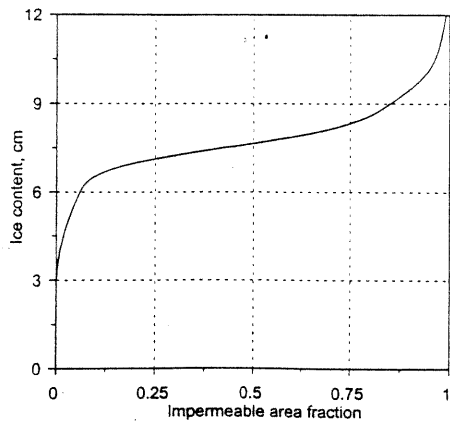


Figure 3. Impermeable area fraction as a function of soil ice content (adapted from Koren [1991]).

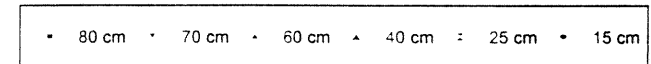
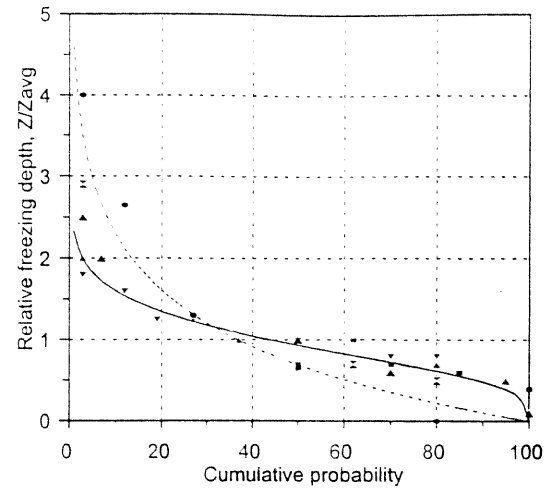


Figure 4. Cumulative gamma distribution functions of the frozen depth  $Z$ , generated using different coefficients of variation: 0.45 (solid line) and 1.0 (dashed line). Symbols represent empirical functions estimated from different spatial average frozen depths,  $Z_{avg}$  (adapted from Koren [1991]).

face runoff  $R_s$ . Once the amount of infiltration is determined, the redistribution of water between soil layers is estimated from (2). As mentioned in section 2.1, the SWB model [Schaake *et al.*, 1996] was adopted to estimate surface runoff:

$$R_s = \frac{P_x^2}{P_x + D[1 - \exp(-K_{dt}\Delta t)]} \quad (19)$$

where  $D$  is the total soil moisture deficit in the rooting zone, and  $K_{dt}$  is a constant. The SWB is a storage type water balance model that accounts for the spatial variability in precipitation and soil moisture storage of the root zone. The model does not, however, account for the effects of frozen ground. Frozen soil is generally less permeable than unfrozen soil, even though it can infiltrate as much water as unfrozen soil under certain conditions [Komarov and Makarova, 1973]. Frozen soil is permeable mainly because of large noncapillary pores that exist in its structural aggregates, cracks, dead root passages, worm

Table 1. Parameterization Parameters Used in the Study

Parameter	Value
Saturation water content $\theta_s$ , $\text{cm}^3 \text{cm}^{-3}$	0.48
Saturation soil suction $\Psi_s$ , m	0.072
Saturation hydraulic conductivity $K_w(\theta_s)$ , $\text{m s}^{-1}$	$5.8 \times 10^{-5}$
Soil retention curve parameter $b$	5.30
Field capacity, $\text{cm}^3 \text{cm}^{-3}$	0.30
Wilting point, $\text{cm}^3 \text{cm}^{-3}$	0.19
Rooting depth, m	1.0
Minimum stomatal resistance, $\text{s m}^{-1}$	40
Roughness length, m	0.045
SWB model parameter $K_{dt}$ , $\text{s}^{-1}$	0.5
Critical value of soil ice $W_{cr}$ , mm	150
Ice content distribution parameter $\alpha$	3.0
Snow compaction parameter $C_1$ , $\text{cm}^{-1} \text{h}^{-1}$	0.01
Snow compaction parameter $C_2$ , $\text{cm}^{-3} \text{g}^{-1}$	21.0
Snow distribution parameter $\alpha_s$	2.6
Snow distribution parameter $W_{max}$ , $\text{m}^{-1}$	0.1

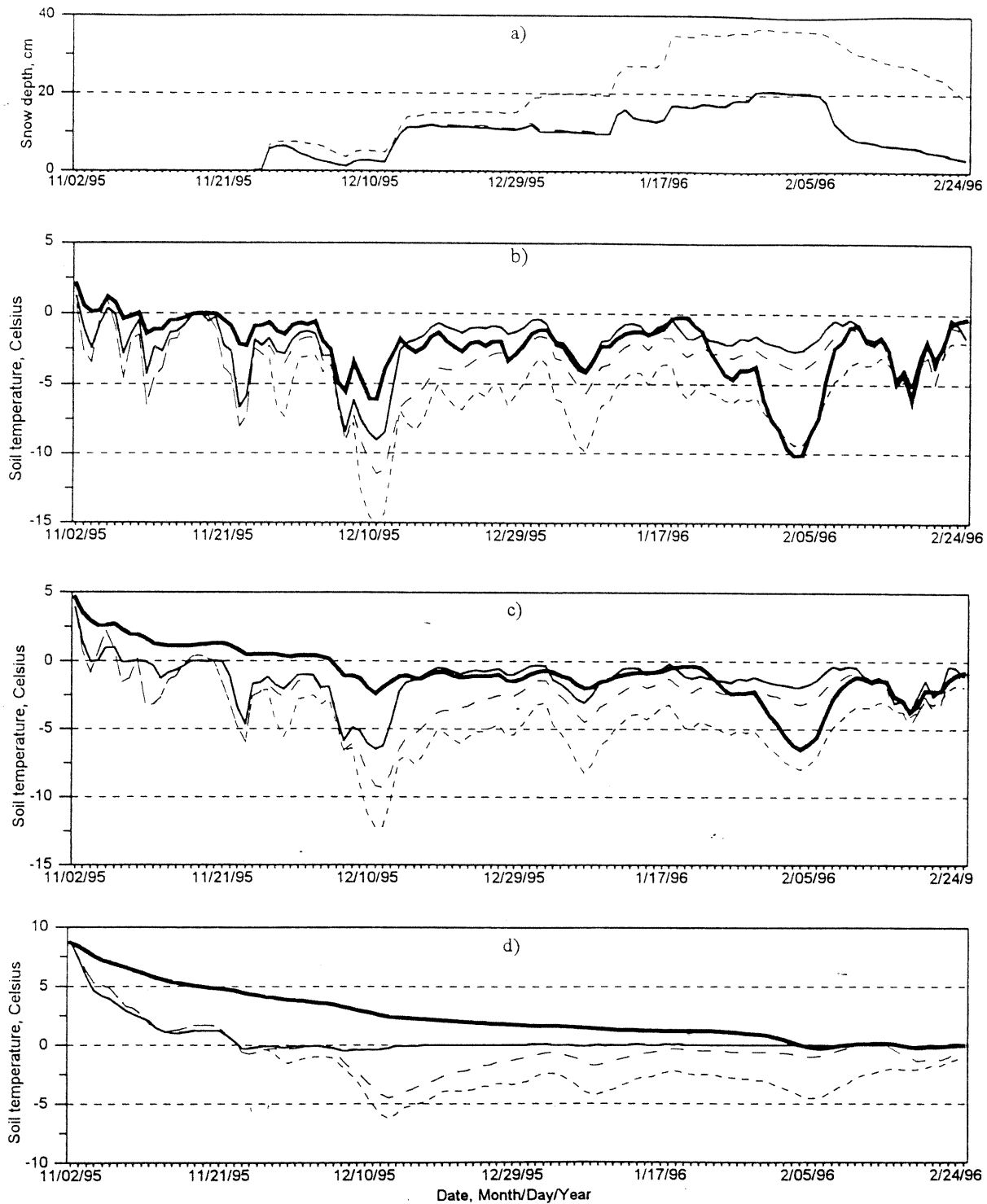


**Figure 5.** (a) Snow depth and soil temperature at the (b) first, (c) second, and (d) third layers estimated from the frozen ground version A (thin solid lines), the nonfrozen ground version B (dashed lines), and the original Eta version C (dotted lines). Observed soil temperature (thick solid lines) is shown at the depths closest to the middle depth of each model layer.

holes, etc. An increase in the ice content can produce completely impermeable soil layers [Komarov, 1957; Emerson, 1994]. We assume that the area where impermeable soil layers are formed produces only direct surface runoff, and the rest of the area produces surface runoff  $R_s^*$ , as calculated by (19). Accordingly, the total areal runoff  $R_s$  is

$$R_s = (1 - F_c)R_s^* + F_c P_x \quad (20)$$

where  $F_c$  is the fraction of impermeable area.

Certain critical conditions of water and heat storage in the soil must exist to have an impermeable layer [Komarov, 1957; Kalyuzhnyy et al., 1978; Sheng et al., 1995]. The water-heat

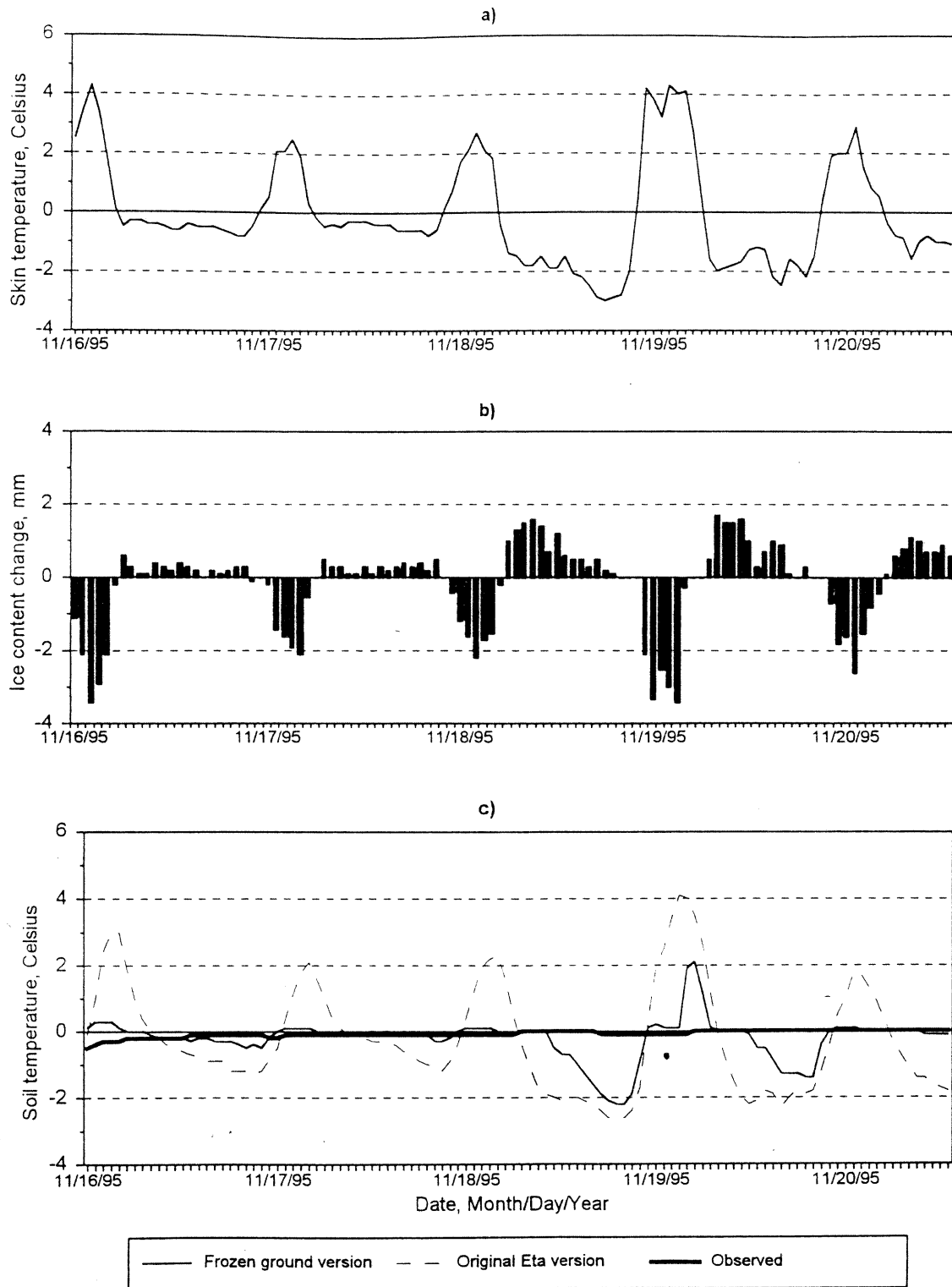
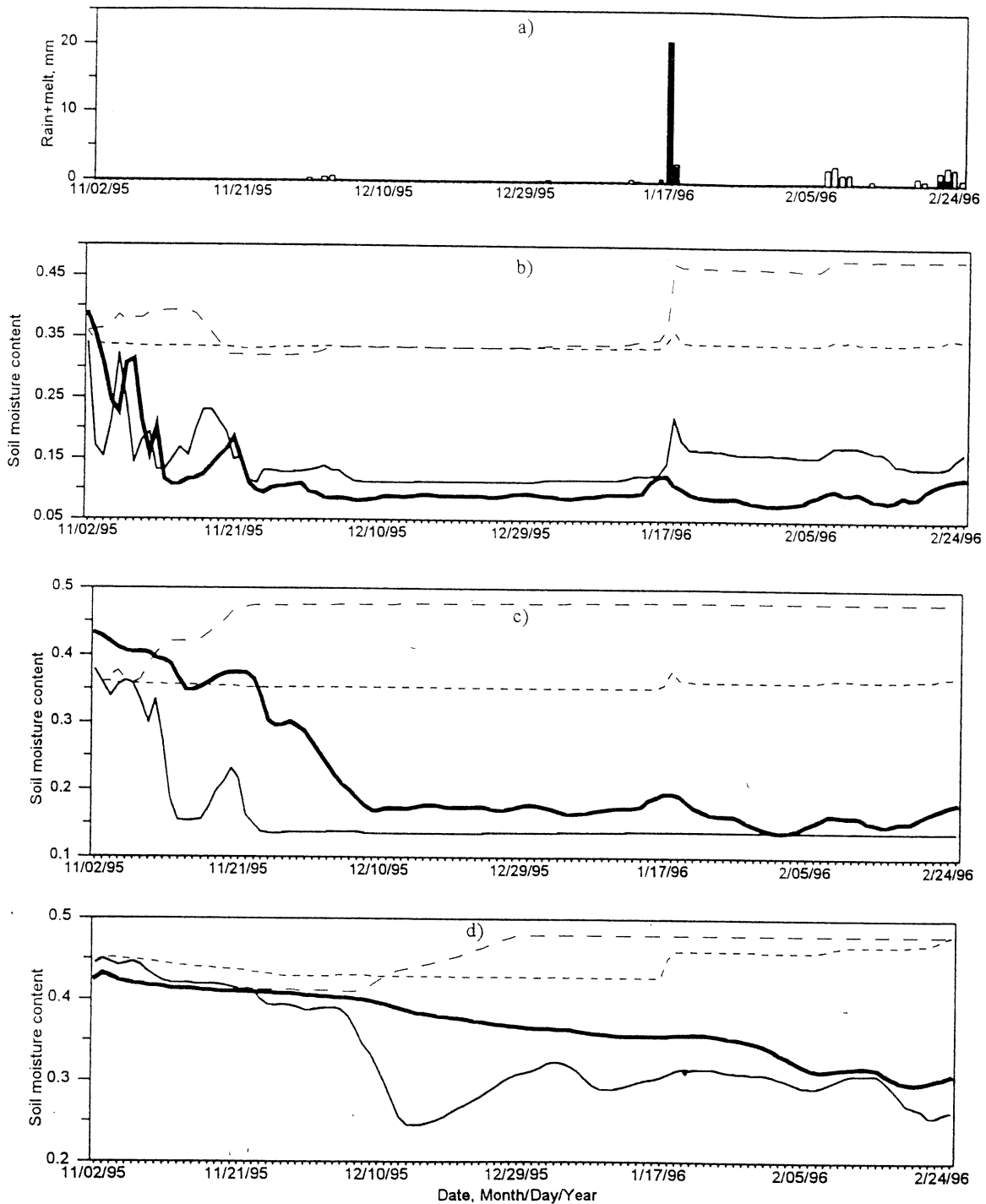


Figure 6. Diurnal cycles of (a) estimated skin temperature, (b) ice content change, (positive when freezing, and negative when thawing), and (c) the first layer soil temperature during snow free surface.

storage varies significantly depending on surface topography and soil characteristics (type, texture, depth, etc.). Field experiments suggest that the spatial extent of an impermeable area depends on the area-averaged ice storage in the frozen soil column [Kapotov, 1976]. An example of such a relationship is shown in Figure 3. Following Koren [1991], it is assumed that

for a particular soil and vegetation there exists a certain critical amount of the soil ice, defined as a depth of water  $W_{cr}$ , above which the soil is practically impermeable. It is also assumed that the spatial variability of soil ice can be described by a probability density function  $f(W_{ice})$  where  $W_{ice}$  is a water equivalent depth. Under these assumptions the fraction of the



**Figure 7.** Simulated snowmelt (white bar) plus (a) rain (black bar), and simulated unfrozen water content from the frozen ground version (a) (thin solid lines), and total soil moisture content from the frozen ground (dashed lines) and the original Eta (dotted lines) versions at the (b) first, (c) second, and (d) third layers. Observed unfrozen water content (thick solid lines) is an average over each model layer.

impermeable area  $F_c$  can be calculated as a probability that soil ice storage is above its critical value

$$F_c\{W_{ice} > W_{cr}\} = 1 - \int_0^{W_{cr}} f(W_{ice}) dW_{ice} \quad (21)$$

There are limited data to develop probability density func-

tions for soil ice. Analysis of experimental data on a few Russian basins suggest that a gamma distribution can be used to approximate empirical distributions of frozen depth and soil moisture content (the soil ice is a product of these two). Figure 4 from Koren [1991] is an example of empirical distribution functions of frozen depth approximated by the gamma function. The figure indicates that lower areal average depths cor-

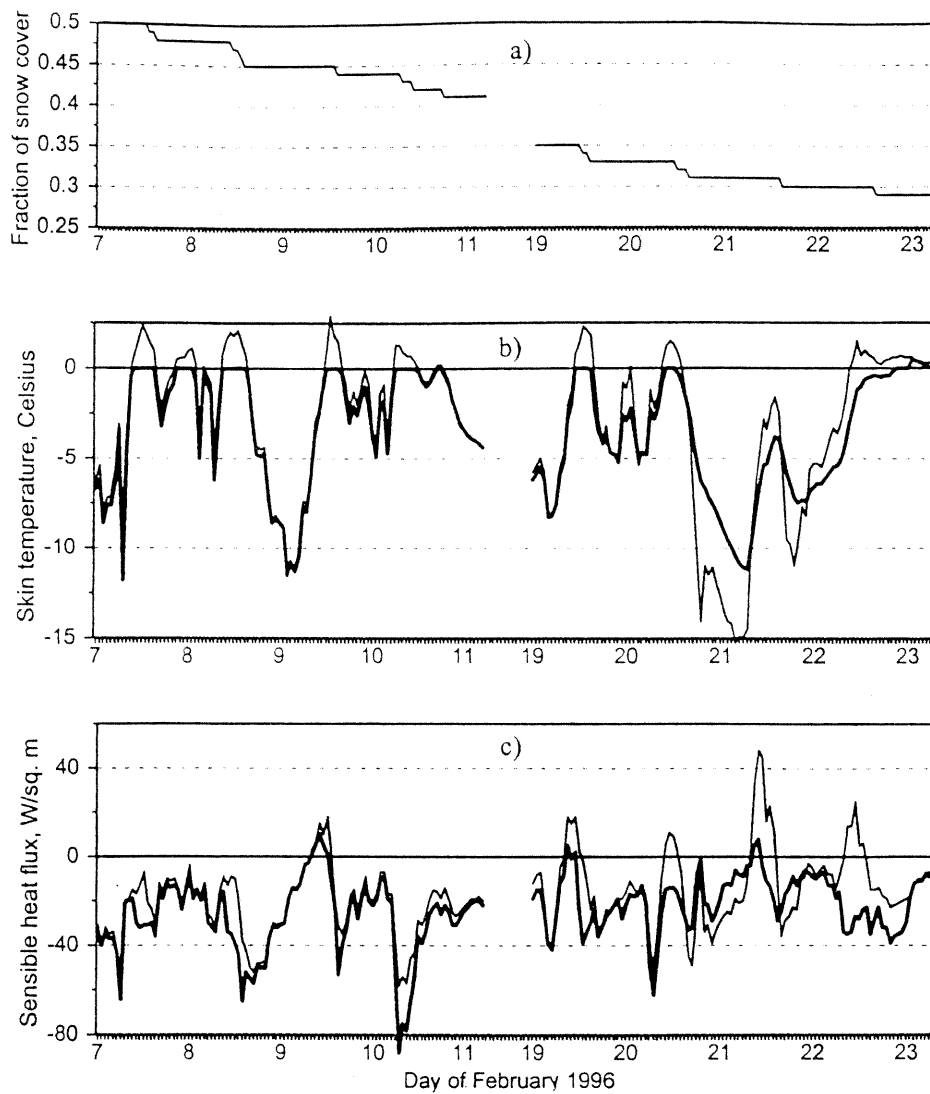


**Figure 8.** Effect of (a) fractional snow cover on (b) skin temperature and (c) sensible heat flux (negative flux means a heat sink to the atmosphere, and positive flux means a heat source to the soil surface) during snowmelt. Results from the new parameterization (solid lines) are plotted against the original Eta parameterization (thick solid lines).

respond to higher spatial variability of frozen depth. If the gamma distribution is used to account for spatial variability of ice content, (21) becomes

$$F_c = \frac{1}{\Gamma(\alpha)} \int_0^v x^{\alpha-1} e^{-x} dx \quad (22)$$

where the upper limit of the integral  $v$  is a function of the gamma distribution parameter  $\alpha = 1/C_v^2$  and the soil ice averaged over the area of interest

$$v = \alpha \frac{W_{cr}}{\bar{W}_{ice}} \quad (23)$$

A more practical expression for  $F_c$  can be obtained by rounding parameter  $\alpha$  to the nearest integer value  $\alpha^*$

$$F_c = e^{-v} \sum_{i=1}^{\alpha^*} \frac{v^{\alpha^*-i}}{\Gamma(\alpha^* - i + 1)} \quad (24)$$

Equations (23) and (24) have two parameters:  $\alpha$  (or  $\alpha^*$ ), which depends on the coefficient of variation of soil ice  $C_v$ , and the critical value of soil ice  $W_{cr}$ . As indicated in Figure 4, just two different values for  $C_v$  cover a wide range of freezing depth scenarios. It is more difficult, however, to estimate parameter  $W_{cr}$  because it is model dependent. Figure 3 provides some guidance for estimating  $W_{cr}$  for clay type soils. It suggests that  $W_{cr}$  is about 120–150 mm in water equivalent, although the exact frozen depth is not clearly defined. Generally higher values of  $W_{cr}$  should be used for sandy soils. Some calibration may be necessary to obtain reliable estimates for surface runoff.

### 3. Rosemount Field Experiment Data and Model Configuration Used

Data from the University of Minnesota were used to test the new snowpack and frozen ground parameterization for Eta-LSS. The Rosemount station is located ~20 km south of St. Paul (44°43'N latitude, 93°05'W longitude, 294 m MSE) on a

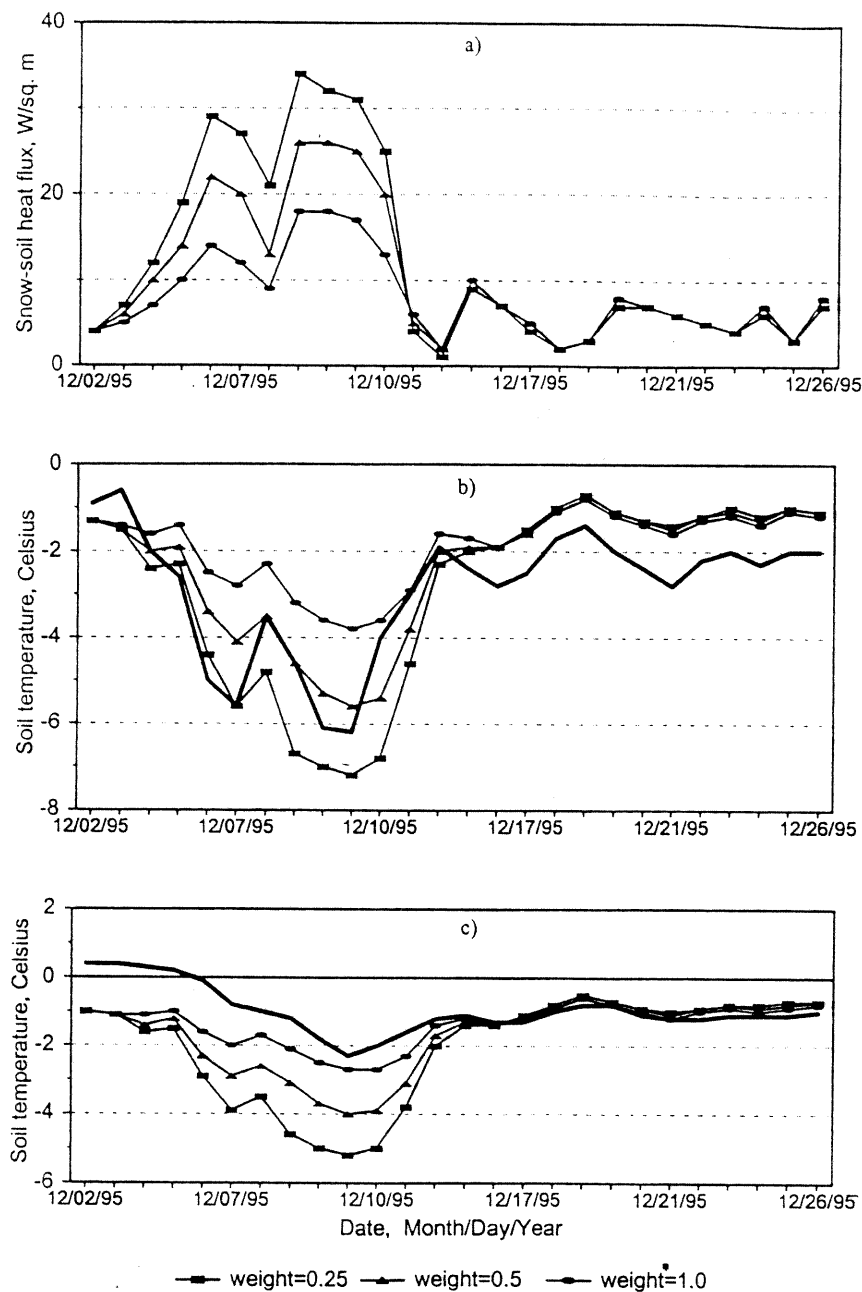


**Figure 9.** (a) Snow-soil heat fluxes and soil temperatures for the (b) first and (c) second layers simulated using different weight fraction  $\zeta$ . Observed soil temperature (thick solid lines) is shown at the depths closest to the middle depth of each model layer.

relatively level glacial outwash plain. The soil at the site is a Waukegan silt loam, for which the physical properties have been extensively characterized [Spaans and Baker, 1995]. All measurements were made at the center of a 17 ha farm field. Soil water content and temperature were measured at eight depths ranging from 2.5 cm to 1 m. Temperatures were measured with precision-calibrated thermistors, and water content was measured with an automated, multiplexed time domain reflectometry (TDR) system [Baker and Allmaras, 1990]. In frozen soil, TDR measures liquid water only. Comprehensive meteorological data were also collected at the site. Measurements were made every 15 s and averaged or totaled at 30 min intervals and included incoming and reflected solar radiation,

incoming and outgoing longwave radiation, temperature, relative humidity, barometric pressure, wind speed, and precipitation.

A four-layer version of Eta-LSS was employed to represent the Waukegan silt loam soil profile at Rosemount. The three root zone layers are defined at 0–10, 10–30, and 30–90 cm depths, respectively. The fourth and bottom soil layer extends from 90 cm to 160 cm. Model parameters controlling water redistribution were estimated on the basis of measured soil properties at the site (soil retention curve, hydraulic conductivity, porosity, etc.). Vegetation-related parameter values were adopted from Chen *et al.* [1996]. Soil- and vegetation-related parameters used in this study are listed in Table 1. Soil temperature at 3 m depth is assumed to be the bottom bound-

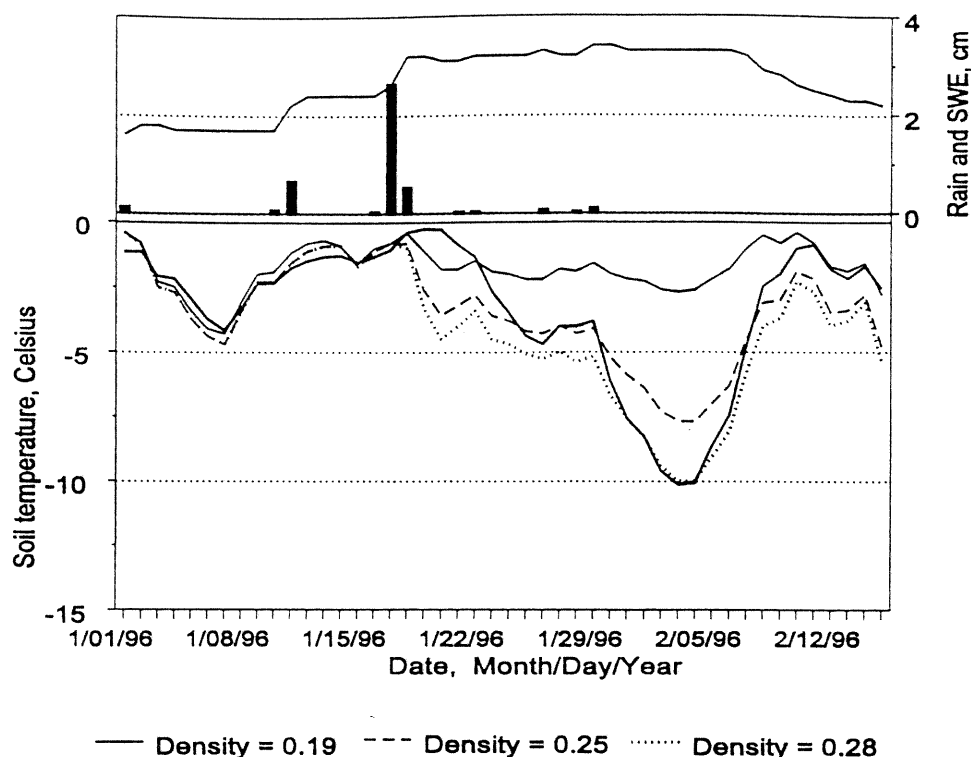


**Figure 10.** Observed (thick solid line) and simulated soil temperatures for the first layer using different snow densities after heavy rain are plotted in the bottom panel. Simulated snow water equivalent (SWE) (solid line) and rainfall (bar) are shown in the top panel.

ary condition. Its value is equal to  $7.5^{\circ}\text{C}$ , the long-term annual air temperature. Initial conditions at four soil layers were estimated from soil moisture contents and temperatures measured at the beginning of October 1995. Simulations were performed continuously to the end of the cold season using a half-hourly time step. Observed values of surface albedo were used in these tests rather than the default values used in the operational Eta model.

#### 4. Test Results and Discussion

##### 4.1. Soil Temperature and Soil Moisture Content Results From Initial Testing

Figure 5 displays mean daily observed and simulated soil temperatures at three top layers during the 1995–1996 cold season. Observed temperatures were selected at the depths closest to the middle depth of each soil layer, namely 5, 20, and 60 cm. Simulated snow depths are also shown in Figure 5a. Each plot presents results for three different versions of Eta-LSS: version A, the new Eta-LSS with both the modified snow component and the frozen ground scheme; version B, the original Eta-LSS with only the modified snow component; and version C, the original Eta-LSS. The results clearly indicate that simulation results using version A are closest to the observed data. Simulated temperatures using version C, the original Eta-LSS, are generally too cold. Results from version B track that of version A closely in the first layer, but differences between them can be as much as  $5^{\circ}$  in the two deeper layers. These results confirm the hypothesis that the latent heat of ice fusion significantly affects soil temperature variability. This can be seen more clearly in Figure 6, which shows hourly soil

temperatures during multiple-freezing/thawing transition periods in the top layer. Although soil surface temperature varies from  $-3^{\circ}\text{C}$  to  $+4^{\circ}\text{C}$  (Figure 6a), version A produces stable soil temperature in the first layer, which matches the observed first layer temperature reasonably well (Figure 6c). The ice content change in the top 30 cm soil layer (Figure 6b) suggests that the heat energy from soil thawing/freezing stabilizes day/night variability in soil temperature. Diurnal variation in soil temperatures from the original Eta-LSS follows the soil surface temperature variation very closely, even during freezing periods. This is not consistent with observed soil temperature.

Figure 7 displays the total and unfrozen soil moisture contents simulated by versions A and C. Version B results are not plotted because they are very similar results of version C. It can be seen clearly from the measurements that liquid soil moisture contents decrease as freezing conditions persist. Version C does not have a frozen water component, and therefore only the total unfrozen water contents are simulated. Results from version A agree reasonably with the measured liquid water contents, although liquid water contents in the second and third layers are somewhat underestimated. The underestimation is due to the deeper than observed penetration of low soil temperatures predicted by the models (see Figure 5). Simulation results from version A suggest that there is a significant upward movement of water during soil-freezing periods. Upward water movement is due to the gradient in water potential created by the abrupt drop in water potential that accompanies freezing in porous media, expressed in (15). This is the driving force that can create frost heave if sufficient water is available in the subsoil to feed continued ice lens growth. It can be seen that the November period experienced a substantial increase in

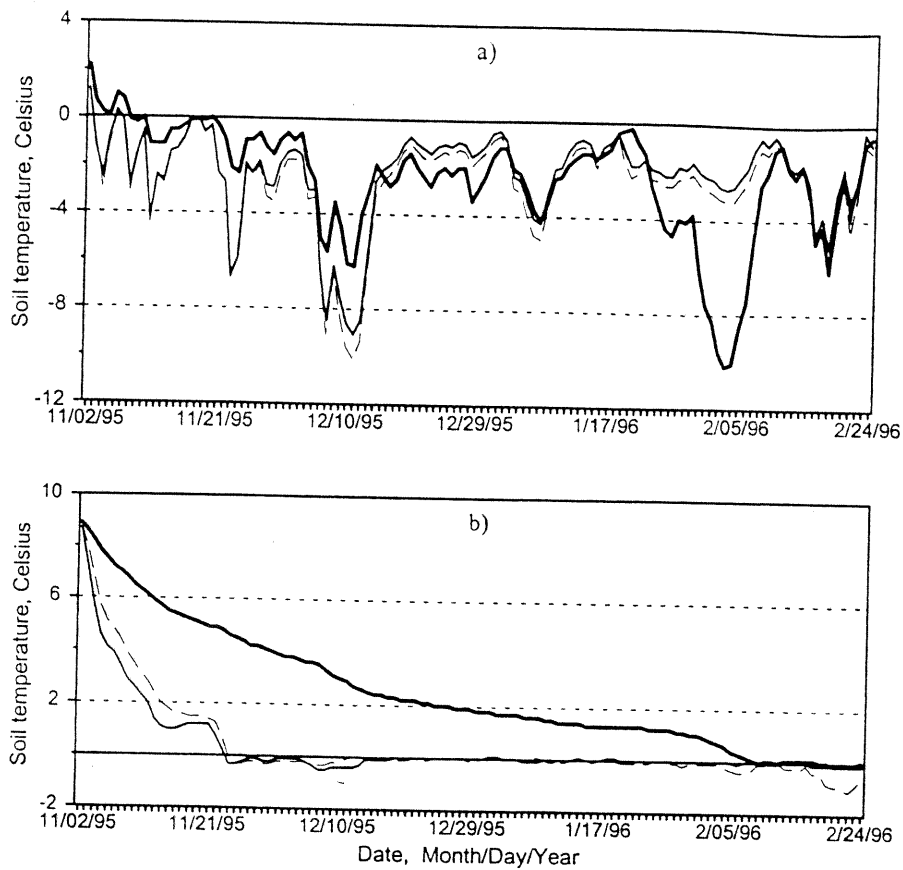


**Figure 11.** Observed (thick solid lines) and simulated soil temperatures for the (a) first and (b) third layers using McCumber and Pielke (thin solid lines) and Johansen's (dashed lines) formulations of soil thermal conductivity.

total soil moisture in the top two layers and, similarly, during the December period for the third layer, reflecting that the most intensive soil-freezing activities occurred in this period. The hydrological impact of frozen ground can be seen from the total soil moisture contents in early February, before spring snowmelt occurred. After intense rain on snow on January 17, soil water content in the first layer from version A was increased dramatically. At the same time, version C generated only minor increase in soil moisture content in the first layer. Most rainwater was percolated into deeper soil layers. Differences in total soil moisture estimated from versions A and C can be as much as 20–25%. It means that version C would have less water available for evaporation and generate less runoff in the spring.

The effect of fractional snow cover on skin temperature and sensible heat flux of a unified snow-bare soil surface can be seen in Figure 8. Fraction of snow cover, skin temperature, and sensible heat flux from versions A and C are plotted for two snowmelt periods in February 1996. Skin temperature from the original Eta-LSS is kept at 0°C during snowmelt periods, although the fraction of snow cover was less than 0.5. As a result, sensible heat flux from this version was much less as compared to the new parameterization results. These differences were greater when the snow cover fraction dropped down below 0.35–0.30.

#### 4.2. Parameterization Evaluation and Sensitivity Tests

Although version A shows a significant improvement over version C, the results show some problems in both the new and the original versions. This can be illustrated by two events from

Figures 5 and 7: significant underestimation of soil temperatures in December for all versions, and overestimation of soil temperatures at the end of January for the new version.

The first case can be attributed to the way in which the heat flux between snow and soil surface is parameterized in the original Eta-LSS. The heat flux is estimated as a function of the gradient between the snow surface temperature (skin temperature) and the soil surface temperature. Because the soil surface temperature is not directly modeled, simulated soil temperature in the top layer is used as its replacement. This implies an isothermal top soil layer, which is good assumption only under moderate or deep snowpack but is a poor assumption under shallow snowpack. The new Eta-LSS also adopted this assumption. This assumption can result in significant errors in estimating the snow-soil surface heat flux when the snow cover is shallow as compared to the thickness of the top soil layer. The December event was characterized by a shallow snow depth, which was below 1 cm.

A sensitivity test was performed on this event. The soil surface temperature  $T_{\text{soil}}$  was estimated as a weighted value between the skin temperature  $T_{\text{skin}}$  and the top layer soil temperature  $T_1$ :

$$T_{\text{soil}} = \omega T_{\text{skin}} + (1 - \omega) T_1 \quad (25)$$

where weight  $\omega$  is dependent on the ratio between the snow depth  $H$  and the top soil layer thickness  $\Delta z_1$

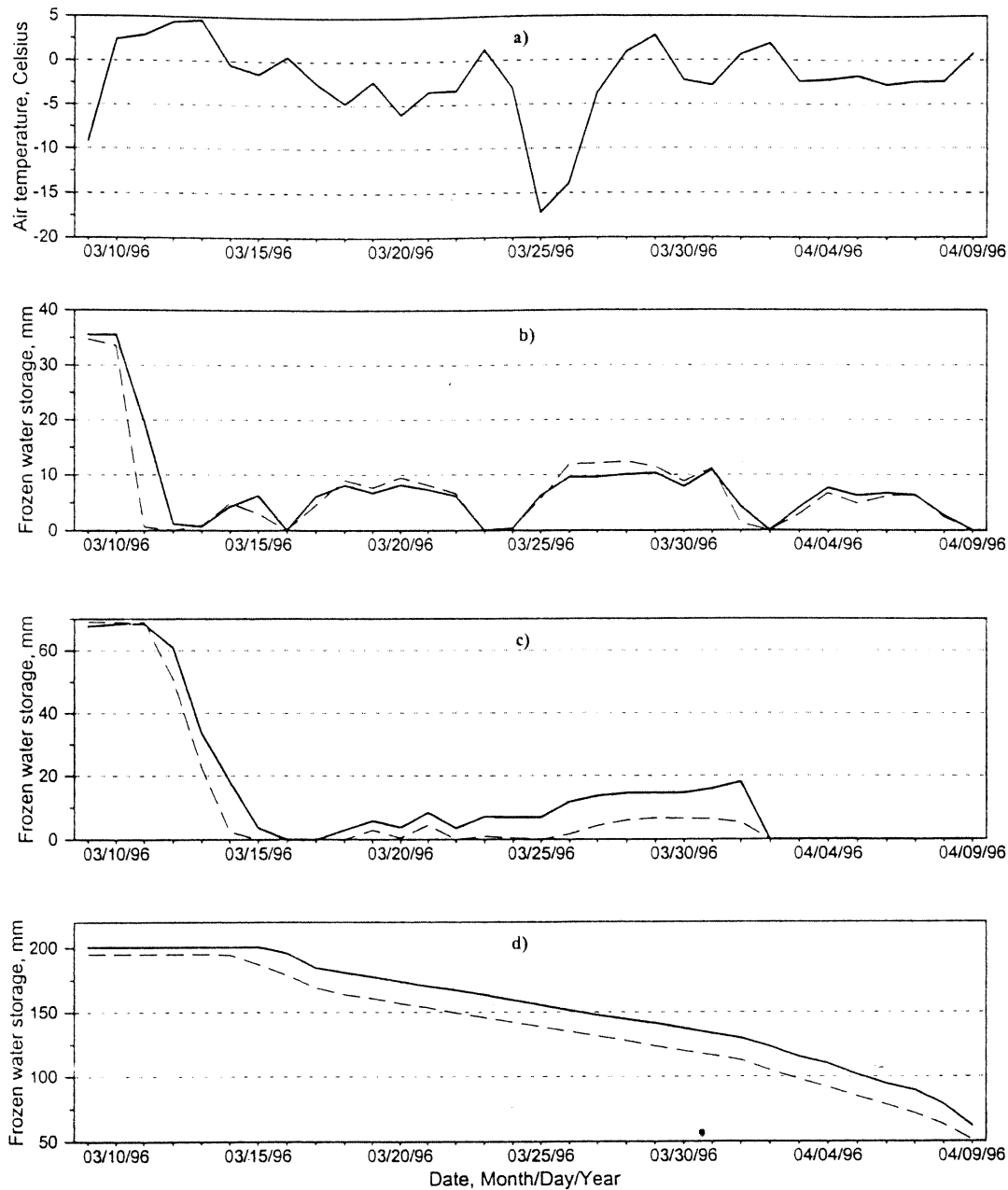


**Figure 12.** Model sensitivity to the number of soil layers. Frozen soil water storages from 10-layer (solid lines) and 4-layer (dashed lines) versions are plotted for three layers: (b) 0–10 cm, (c) 10–30 cm, and (d) 30–90 cm. Observed air temperature is also shown in the plot (Figure 1a).

$$\omega = \frac{0.5\zeta\Delta z_1}{H + 0.5\zeta\Delta z_1} \quad (26)$$

Here  $\zeta$  can vary from zero (according to the original Eta-LSS) to infinity (i.e., no heat exchange between snow and soil). We tested the values of 0.25, 0.50, and 1.00 for  $\zeta$ . The correction was applied when snow depth was less than 2.5 cm (half of the soil depth where top layer temperature is estimated). Results of this test are presented in Figure 9. The figure clearly shows that simulated soil temperatures in the two top layers are quite sensitive to differences in the estimation of heat flux. The larger the  $\zeta$  used, the lower the snow-soil surface heat flux (Figure 9a) and soil temperature (Figures 9b and 9c) are simulated.

The second event, overestimation of soil temperatures in

January, seems to be related to how snow density and thermal conductivity are estimated in the new Eta-LSS. A total of 36 mm of heavy rain fell on snow during January 16–17. Simulated snow density was  $0.17 \text{ g cm}^{-3}$  at the beginning of rain and  $0.19 \text{ g cm}^{-3}$  at the end. Although the snow parameterization accounts for snow compaction during snowmelt, it does not account for snow destruction during rainfall. Actual snow density can be much higher after heavy rain. If snowpack holds, for example, 10% of liquid water, snow density would be as much as  $0.25 \text{ g cm}^{-3}$ . Figure 10 displays the results for test cases when the snow density was increased to 0.25 and  $0.28 \text{ g cm}^{-3}$ , respectively, to account for effects of heavy rain. The figure indicates that simulated snow-soil surface flux is very sensitive

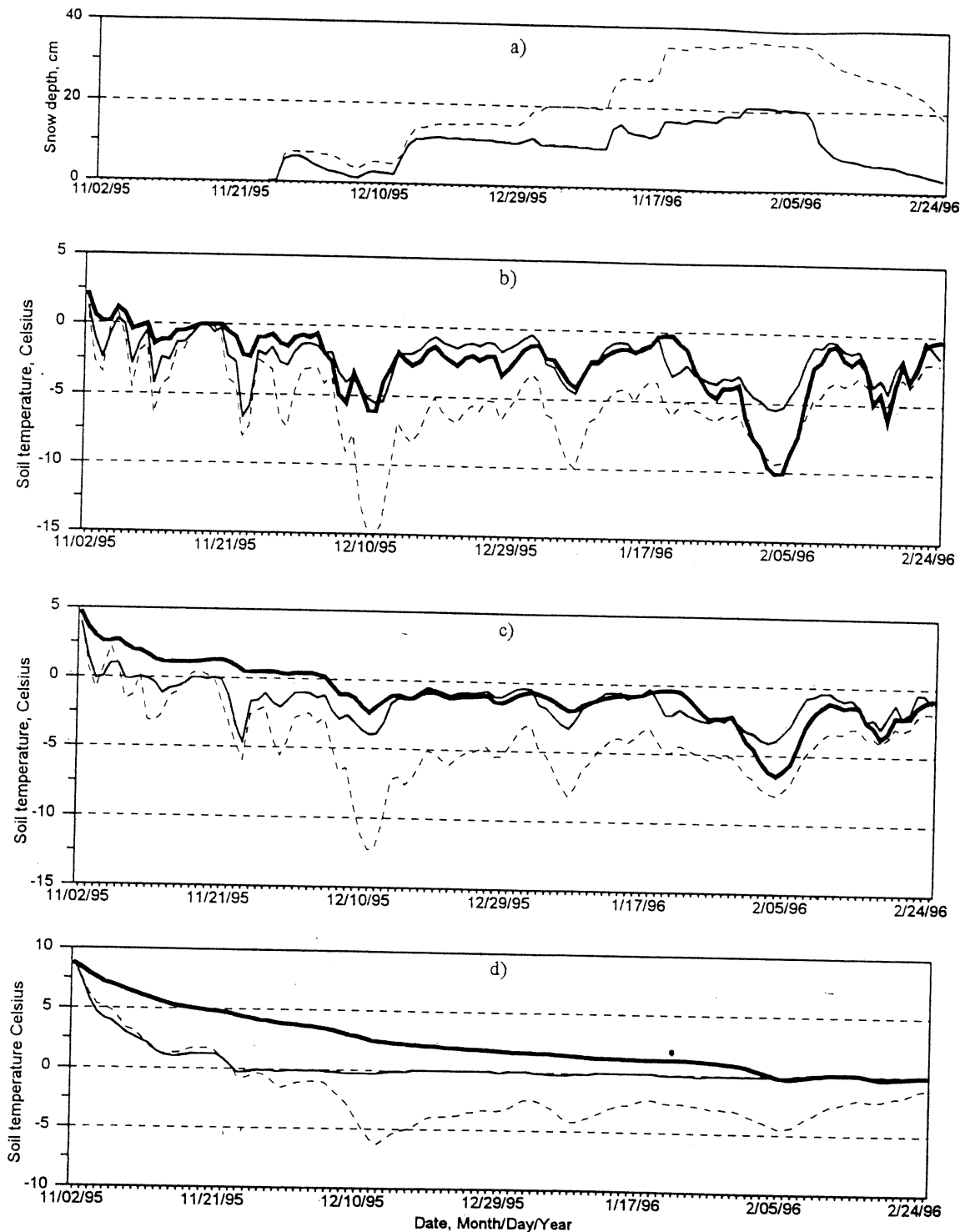


**Figure 13.** (a) Snow depth and soil temperature at the (b) first, (c) second, and (d) third layers estimated from the modified frozen ground version (thin solid lines) and the original Eta version (dotted lines). Observed soil temperature (thick solid lines) is shown at the depths closest to the middle depth of each model layer.

to snow density when it is above  $0.2\text{--}0.22\text{ g cm}^{-3}$ . This is because most empirical formulas have exponential type relationships for snow density and snow thermal conductivity. A change in snow density from  $0.19$  to  $0.25\text{ g cm}^{-3}$  can result in as much as  $5^\circ$  in soil temperature change in the top soil layer. Therefore a more robust approach to estimating snow density

and snow thermal conductivity should be considered for improved model performance.

Soil thermal conductivity parameterization may be another source of uncertainties in estimating soil heat fluxes. *Peters-Lidard et al.* [1998] analyzed Johansen's soil thermal conductivity parameterization [Farouki, 1986] as well as that of *Mc-*

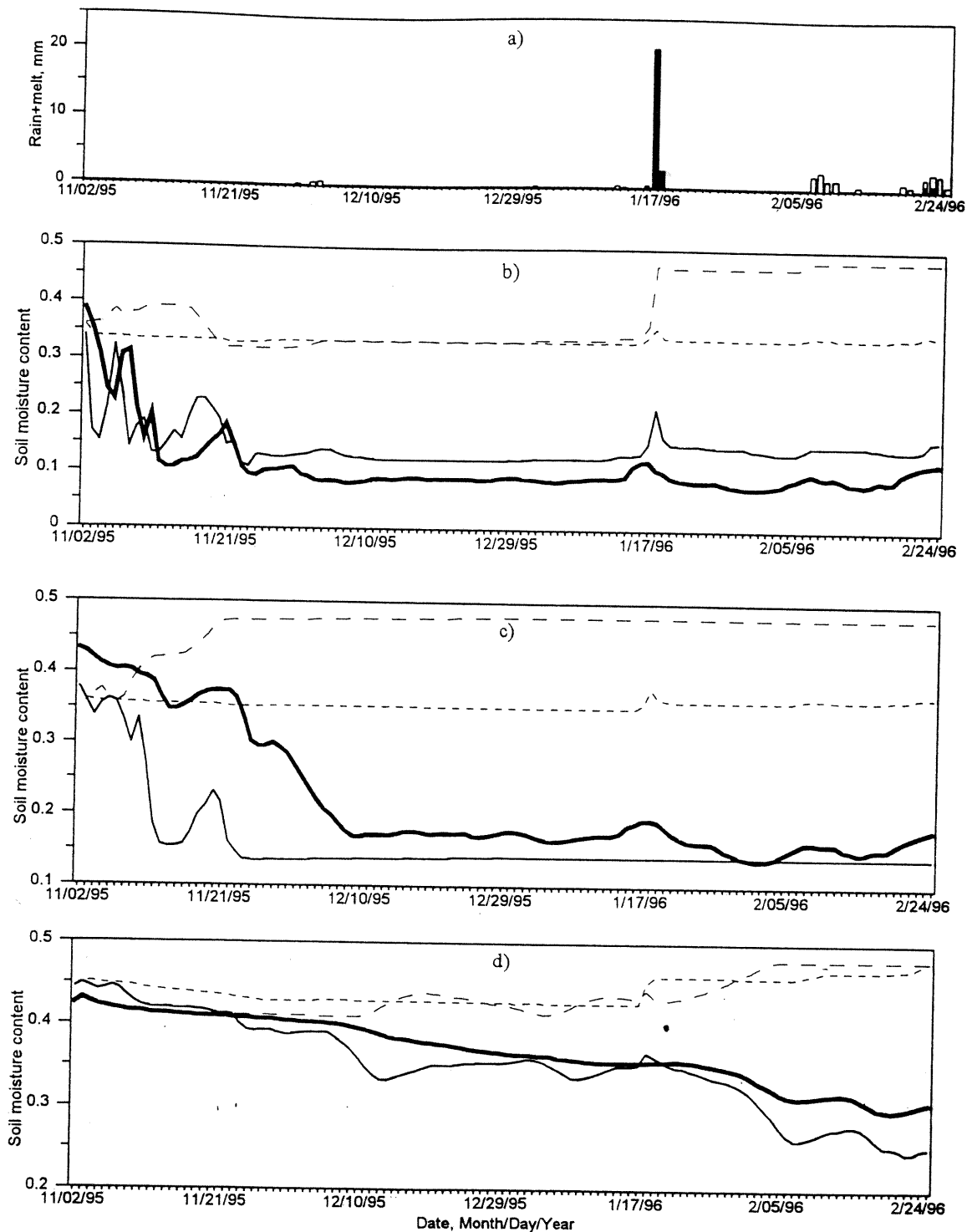


**Figure 14.** (a) Simulated snowmelt (white bar) plus rain (black bar) and simulated unfrozen water content from the modified frozen ground version (thin solid lines) and total soil moisture content from the modified frozen ground (dashed lines) and original Eta (dotted lines) versions at the (b) first; (c) second, and (d) third layers. Observed unfrozen water content (thick solid lines) is an average over each model layer.

Cumber and Pielke [1981]. They concluded that the formulation of McCumber and Pielke (which is used in the Eta model parameterization) usually overestimates soil thermal conductivity at high soil moisture contents and underestimates at low soil moisture contents. To estimate the effect of soil thermal conductivity formulation on Rosemount simulation

results, a parallel run using the Johansen formulation was performed. Quartz content for the silt loam soil was estimated on the basis of the recommendation from Peters-Lidard *et al.* [1998]. Figure 11 displays simulated soil temperatures in the first and third layers using both formulations. During this particular simulation period, soil moisture content was very high.

Surprisingly, the differences between soil temperatures simulated using both formulations were small as compared to their deviations from measured data. The reason for similar performance by both formulations is that the original Eta-LSS applies a very stringent upper limit on McCumber and Pielke's estimation of soil thermal conductivity. Since the Johansen formulation does not need this extra constraint and its parameters can be easily estimated from soil characteristics [Peters-Lidard et al., 1998], it should be considered as a good substitute for the McCumber and Pielke formulation for soil thermal conductivity.

The number of modeled soil layers can also contribute to the model performance. Mahrt and Pan [1984] compared simulation results from a two-layer original Eta-LSS version of the soil moisture parameterization (2) and a high-resolution model developed by Boersma et al. [1983] during a warm period. They concluded that the two-layer model will typically underestimate the water fluxes. However, the impact of such errors on interfacial water flux can be minimized by choosing a sufficiently thin upper soil layer. Soil profile resolution may also affect the phase change processes in soils, specifically during snowmelt. Sensitivity tests were performed with increased number of soil layers. Frozen water storage in the three soil layers, 0–10, 10–30, and 30–90 cm, from 10- and 4-layer versions is plotted in Figure 12. Soil layer thicknesses of the 10-layer version were defined as 5, 5, 5, 5, 10, 10, 20, 20, and 70 cm. Simulations were performed at the end of a snowmelt period when very intensive soil thawing occurred. It can be seen from Figure 12 that the four-layer version leads to slightly faster thawing in the top 30 cm layer as compared to the 10-layer version. However, these differences are probably small compared to the differences that resulted from uncertainties in the representation of soil properties.

#### 4.3. Final Test Results After Corrections

This section presents final model results that embrace the lessons learned from the sensitivity runs of section 4.2. The model simulations in this section used equations (25) and (26) to estimate soil surface temperature when a snow depth less than 2.5 cm existed, and therein a fixed value of 0.5 was used for the weight fraction  $\zeta$ . Additionally, the correction for heavy rain was included in the snow density simulation, whereby in heavy rain exceeding 10% of the snow water equivalent, the snow density was increased to  $0.24 \text{ g cm}^{-3}$ . Results of these simulations are shown in Figures 13 and 14. Results from the original Eta model are also plotted in the figures.

These final simulation results agree better with measured data in both soil temperatures (Figure 13) and soil moisture contents (Figure 14), specifically during December and January events. The dynamics of unfrozen soil moisture content for the third layer was improved significantly.

### 5. Conclusions and Future Studies

Simulation results for Rosemount, Minnesota, showed significant effects of cold season processes on both soil temperature and soil moisture distribution. The new Eta-LSS outperformed the original Eta-LSS when compared to observed data. The total soil moisture content at the end of winter estimated by the new Eta-LSS can be 20–25% higher than that estimated by Eta-LSS without frozen ground component. Differences in soil temperatures can be as much as 5–8°. Test results also indicate that heat and water fluxes are very sensitive to uncer-

tainties in soil surface boundary conditions and to variation in thermal conductivities of snow and soil.

Rosemount experimental data have provided only limited tests of the new Eta-LSS. More extensive tests are planned using data from river basins where seasonal snow cover exists and where frozen ground has a substantial effect on runoff generation.

**Acknowledgments.** This work was part of the NWS/NCEP GCIP Core Project supported by NOAA's Office of Global Programs. The authors gratefully acknowledge the helpful comments of two anonymous reviewers.

### References

- Anderson, E., National Weather Service River Forecast System—Snow Accumulation and Ablation Model, *NOAA Tech. Memo., NWS HYDRO-17*, U.S. Dep. of Comm., Natl. Oceanic and Atmos. Admin., Washington, D. C., 1973.
- Anderson, E., A point energy and mass balance model of a snow cover, *NOAA Tech. Rep. NWS 19*, Natl. Oceanic and Atmos. Admin., Washington, D. C., 1976.
- Baker, J. M., and R. R. Allmaras, System for automating and multiplexing soil moisture measurement by time-domain reflectometry, *Soil Sci. Soc. Am. J.*, 54, 1–6, 1990.
- Barnett, T. P., L. Dumenil, U. Schlese, E. Roeckner, and M. Latif, The effect of Eurasian snow cover on regional and global climate variations, *J. Atmos. Sci.*, 46, 661–685, 1989.
- Bergstrom, S., Development of a snow routine for the HBV-2 model, *Nord. Hydrol.*, 6(2), 73–92, 1975.
- Betts, A., F. Chen, K. Mitchell, and Z. Janjic, Assessment of the land surface and boundary layer models in two operational versions of the NCEP Eta model using FIFE data, *Boundary Layer Meteorol.*, 125, 2896–2916, 1997.
- Black, T. L., The new NMC mesoscale Eta model: Description and forecast examples, *Weather Fore.*, 9(2), 265–278, 1994.
- Boersma, L., M. J. Unga, and E. L. McCoy, Transfer problems in soils, in *Proceedings of the World Congress on Systems Simulation and Scientific Computation*, Int. Assoc. for Math. and Comput. in Simul., 8–13 August, Montreal, Ont., Canada, 1983.
- Campbell, G. S., A simple method for determining unsaturated conductivity from moisture retention data, *Soil Sci.*, 117, 311–314, 1974.
- Chen, F., K. Mitchell, J. Schaake, Y. Xue, H.-L. Pan, V. Koren, Q. Y. Duan, M. Ek, and A. Betts, Modeling of land surface evaporation by four schemes and comparison with FIFE observations, *J. Geophys. Res.*, 101, 7251–7268, 1996.
- Chen, F., Z. Janjic, and K. Mitchell, Impact of atmospheric surface-layer parameterizations in the new land-surface scheme of the NCEP mesoscale Eta model, *Boundary Layer Meteorol.*, 85, 391–421, 1997.
- Cosby, B. J., G. M. Hornberger, R. B. Clapp, and T. R. Ginn, A statistical exploration of the relationships of soil moisture characteristics to the physical properties of soils, *Water Resour. Res.*, 20, 682–690, 1984.
- DeGaetano, A. T., D. S. Wilks, and M. McKay, A physically based model of soil freezing in humid climates using air temperature and snow cover data, *J. Appl. Meteorol.*, 35(6), 1009–1027, 1996.
- Dickinson, R. E., A. Henderson-Sellers, and P. J. Kennedy, Biosphere-Atmosphere Transfer Scheme (BATS) version 1e as coupled to the NCAR Community Climate Model, *NCAR Tech. Note, NCAR/TN-387+STR*, 20 pp., Natl. Cent. for Atmos. Res., Boulder, Colo., 1993.
- Ek, M., and L. Mahrt, *OSU 1-D PBL Model User's Guide*, Dep. of Atmos. Sci., Oreg. State Univ., Corvallis, 1991.
- Emerson, D. G., Movement of water in seasonally frozen soil, Southeastern North Dakota, 1985–87, *U.S. Geol. Surv., Water Resour. Invest. Rep. 92-4110*, North Dakota State Water Comm., Bismarck, 32 pp., 1992.
- Engelmark, H., and U. Svensson, Numerical modelling of phase change in freezing and thawing unsaturated soil, *Nord. Hydrol.*, 24, 95–110, 1993.
- Farouki, O., *Thermal Properties of Soils*, vol. 11, in *Series of Rock and Soil Mechanics*, Trans. Tech. Publ., Clausthal-Zellerfeld, Germany, 1986.

- Flerchinger, G. N., and K. E. Saxton, Simultaneous heat and water balance model of a freezing snow-residue-soil system, I, Theory and development, *Trans. ASAE*, 32(2), 565-571, 1989.
- Foster, J., G. Liston, R. Koster, R. Essersy, H. Behr, L. Dumenil, D. Versegny, S. Tompson, D. Pollard, and J. Cohen, Snow cover and snow mass intercomparisons of general circulation models and remotely sensed data sets, *J. Clim.*, 9, 409-426, 1996.
- Fuchs, M., G. S. Campbell, and R. I. Papendick, An analysis of sensible and latent heat flow in a partially frozen unsaturated soil, *Soil Sci. Soc. Am. J.*, 42(3), 379-385, 1978.
- Fukuda, M., and T. Ishizaki, General report on heat and mass transfer, *Proc. Symp. Ground Freezing*, 2, 409-416, 1992.
- Gottlib, L., A general runoff model for snow-covered and glacierized basins, *Nord. Hydrol. Conf.*, 6, 172-177, 1980.
- Gutman, G., and A. Ignatov, The derivation of the green vegetation fraction from NOAA/AVHRR data for use in numerical weather prediction models, *Int. J. Remote Sens.*, 19(8), 1533-1543, 1998.
- Harlan, R. L., Analysis of coupled heat-fluid transport in partially frozen soil, *Water Resour. Res.*, 9(5), 1314-1323, 1973.
- Jacquemin, B., and J. Noilhan, Sensitivity study and validation of a land surface parameterization using the HAPEX-MOBILHY data set, *Boundary Layer Meteorol.*, 52, 93-134, 1990.
- Janjic, Z. I., The step-mountain Eta coordinate: Further development of the convection, viscous sublayer, and turbulence closure schemes, *Mon. Weather Rev.*, 122, 927-945, 1994.
- Jarvis, P. G., The interpretation of the variation in leaf water potential and stomatal conductance found in canopies in the field, *Philos. Trans. R. Soc. London, Ser. B*, 273, 593-610, 1976.
- Kalyuzhny, I. L., N. S. Morozova, and K. K. Pavlova, Phase composition of water in the frozen soils of the Vyatka River basin, *Sov. Hydrol.*, 17(4), 255-260, 1978.
- Kane, D. L., and J. Stein, Water movement into seasonally frozen soils, *Water Resour. Res.*, 19(6), 1547-1557, 1983.
- Kapotov, A. A., Estimation of runoff losses on infiltration during spring flood (in Russian), *Proc. 4th Natl. Hydrol. Assem.*, 6, 137-144, 1976.
- Kojima, K., Densification of seasonal snow cover, physics of snow and ice, *Proc. Int. Conf. Low Temp. Sci.*, 1(2), 929-952, 1967.
- Komarov, V. D., Laboratory experiments on the frozen soil infiltration (in Russian), in *Proceedings of the Central Institute of Forecasts*, vol. 54, pp. 3-42, Gidrometeoizdat, Moscow, 1957.
- Komarov, V. D., and T. T. Makarova, Effect of the ice content, temperature, cementation, and freezing depth of the soil on meltwater infiltration in a basin, *Sov. Hydrol.*, 3, 243-249, 1973.
- Koren, V. I., *Mathematical Modeling and Forecasting of River Runoff*, Gidrometeoizdat (in Russian), 200 pp., St. Petersburg, Russia, 1991.
- Kulik, V. Y., *Water Infiltration Into Soil* (in Russian), 93 pp., Gidrometeoizdat, Moscow, 1978.
- Kutchment, L. S., V. N. Demidov, and Y. G. Motovilov, *River Runoff Generation* (in Russian), Russ. Acad. of Sci., Moscow, 1983.
- Leese, J. A., Major activities plan for 1998, 1999 and outlook for 2000 for the GEWEX Continental-Scale International Project (GCIP), *IGPO Publ. Ser.*, 26, Int. GEWEX Proj. Off., NASA, 1997.
- Levine, E. R., and R. G. Knox, Modeling soil temperature and snow dynamics in northern forests *J. Geophys. Res.*, 102, 29,407-29,416, 1997.
- Lunardini, V. J., Heat conduction with freezing or thawing, *CRREL Monogr. 88-1*, U.S. Army Corps of Eng., Wash., D. C., 1988.
- Lynch-Stieglitz, M., The development and validation of a simple snow model for the GISS GCM, *J. Clim.*, 7(12), 1842-1855, 1995.
- Mahfouf, J., and J. Noilhan, Comparative study of various formulations of evaporation from bare soil using in situ data, *J. Appl. Meteorol.*, 30, 1354-1365, 1991.
- Mahrt, L., and K. Ek, The influence of atmospheric stability on potential evaporation, *J. Clim. Appl. Meteorol.*, 23, 222-234, 1984.
- Mahrt, L., and H. L. Pan, A two-layer model of soil hydrology, *Boundary Layer Meteorol.*, 29, 1-20, 1984.
- Marshall, S., J. O. Roads, and G. Glatzmaier, Snow hydrology in a general circulation model, *J. Clim.*, 7(8), 1251-1269, 1994.
- McCumber, M. C., and R. A. Pielke, Simulation of the effects of surface fluxes of heat and moisture in a mesoscale numerical model, *J. Geophys. Res.*, 86, 9929-9938, 1981.
- McPherson, R. D., The National Centers for Environmental Prediction: Operational climate, ocean, and weather prediction for the 21st century, *Bull. Am. Meteorol. Soc.*, 75(3), 363-373, 1994.
- Ming, J., A. Kumar, and A. Leetmaa, A multiseason climate forecast system at the National Meteorological Center, *Bull. Am. Meteorol. Soc.*, 75(4), 569-577, 1994.
- Motovilov, Y. G., Model of snow cover formation and snowmelt processes, *LAHS Publ.*, 155, pp. 47-57, Wallingford, England, 1986.
- Namias, J., Some empirical evidence for the influence of snow cover on temperature and precipitation, *Mon. Weather Rev.*, 113, 1542-1553, 1985.
- O'Neill, K., The physics of mathematical frost heave models: A review, *Cold Reg. Sci. Technol.*, 6, 275-291, 1983.
- Pan, H.-L., and L. Mahrt, Interaction between soil hydrology and boundary-layer development, *Boundary Layer Meteorol.*, 38, 185-202, 1987.
- Peters-Lidard, C. D., E. Blackburn, X. Liang, and E. F. Wood, The effect of soil thermal conductivity parameterization on surface energy fluxes and temperatures, *J. Atmos. Sci.*, 55, 1209-1223, 1998.
- Schaake, J. C., V. I. Koren, Q.-Y. Duan, K. Mitchell, and F. Chen, Simple water balance model for estimating runoff at different spatial and temporal scales, *J. Geophys. Res.*, 101, 7461-7475, 1996.
- Schlosser, C. A., A. Robock, K. Y. Vinnikov, N. A. Speranskaya, and Y. Xue, 18-year land surface hydrology model simulations for a midlatitude grassland catchment in Valday, Russia, *Mon. Weather Rev.*, 125, 3279-3296, 1997.
- Sheng, D., K. Axelsson, and S. Knutsson, Frost heave due to ice lens formation, *Nord. Hydrol.*, 26, 125-146, 1995.
- Spaans, E. J. A., and J. M. Baker, The soil freezing characteristic: Its measurement and similarity to the soil moisture characteristic, *Soil Sci. Soc. Am. J.*, 60, 13-19, 1996.
- Taylor, G. S., and J. N. Luthin, Numeric results of coupled heat-mass flow during freezing and thawing, paper presented at the 2nd Conference on Soil Water Problems in Cold Regions, Nat. Resour. Council, Edmonton, Alta., Canada, September 1-2, 1976.
- Versegny, D. L., CLASS—A Canadian land surface scheme for GCMs, I. Soil model, *Int. J. Climatol.*, 11, 111-133, 1991.
- Yeh, T. C., R. Wetherald, and S. Manabe, A model study of short term climatic and hydrological effects of sub-snow cover removal, *Mon. Weather Rev.*, 111, 1013-1024, 1983.
- J. M. Baker, University of Minnesota, USDA-ARS, DSWC, St. Paul, MN 55108.
- F. Chen, National Center for Atmospheric Research, Boulder, CO 80307.
- Q.-Y. Duan, V. Koren, and J. Schaake, Office of Hydrology, National Weather Service, NOAA, 1325 East-West Highway, Silver Spring, MD 20910. (victor.koren@noaa.gov)
- K. Mitchell, National Centers for Environmental Prediction, NOAA, Camp Springs, MD 20746.

(Received September 11, 1998; revised February 8, 1999; accepted March 25, 1999.)